

First study of antihyperon-nucleon scattering $\bar{\Lambda}p \rightarrow \bar{\Lambda}p$ and measurement of $\Lambda p \rightarrow \Lambda p$ cross section

- M. Ablikim¹, M. N. Achasov^{4,c}, P. Adlarson⁷⁵, O. Afedulidis³, X. C. Ai⁸⁰, R. Aliberti³⁵, A. Amoroso^{74A,74C}, Q. An^{71,58,a}, Y. Bai⁵⁷, O. Bakina³⁶, I. Balossino^{29A}, Y. Ban^{46,h}, H.-R. Bao⁶³, V. Batozskaya^{1,44}, K. Begzsuren³², N. Berger³⁵, M. Berlowski⁴⁴, M. Bertani^{28A}, D. Bettone^{29A}, F. Bianchi^{74A,74C}, E. Bianco^{74A,74C}, A. Bortone^{74A,74C}, I. Boyko³⁶, R. A. Briere⁵, A. Brueggemann⁶⁸, H. Cai⁷⁶, X. Cai^{1,58}, A. Calcaterra^{28A}, G. F. Cao^{1,63}, N. Cao^{1,63}, S. A. Cetin^{62A}, J. F. Chang^{1,58}, G. R. Che⁴³, G. Chelkov^{36,b}, C. Chen⁴³, C. H. Chen⁹, Chao Chen⁵⁵, G. Chen¹, H. S. Chen^{1,63}, H. Y. Chen²⁰, M. L. Chen^{1,58,63}, S. J. Chen⁴², S. L. Chen⁴⁵, S. M. Chen⁶¹, T. Chen^{1,63}, X. R. Chen^{31,63}, X. T. Chen^{1,63}, Y. B. Chen^{1,58}, Y. Q. Chen³⁴, Z. J. Chen^{25,i}, Z. Y. Chen^{1,63}, S. K. Choi^{10A}, G. Cibinetto^{29A}, F. Cossio^{74C}, J. J. Cui⁵⁰, H. L. Dai^{1,58}, J. P. Dai⁷⁸, A. Dbeysi¹⁸, R. E. de Boer³, D. Dedovich³⁶, C. Q. Deng⁷², Z. Y. Deng¹, A. Denig³⁵, I. Denysenko³⁶, M. Destefanis^{74A,74C}, F. De Mori^{74A,74C}, B. Ding^{66,1}, X. X. Ding^{46,h}, Y. Ding³⁴, Y. Ding⁴⁰, J. Dong^{1,58}, L. Y. Dong^{1,63}, M. Y. Dong^{1,58,63}, X. Dong⁷⁶, M. C. Du¹, S. X. Du⁸⁰, Z. H. Duan⁴², P. Egorov^{36,b}, Y. H. Fan⁴⁵, J. Fang^{1,58}, J. Fang⁵⁹, S. S. Fang^{1,63}, W. X. Fang¹, Y. Fang¹, Y. Q. Fang^{1,58}, R. Farinelli^{29A}, L. Fava^{74B,74C}, F. Feldbauer³, G. Felici^{28A}, C. Q. Feng^{71,58}, J. H. Feng⁵⁹, Y. T. Feng^{71,58}, M. Fritsch³, C. D. Fu¹, J. L. Fu⁶³, Y. W. Fu^{1,63}, H. Gao⁶³, X. B. Gao⁴¹, Y. N. Gao^{46,h}, Yang Gao^{71,58}, S. Garbolino^{74C}, I. Garzia^{29A,29B}, L. Ge⁸⁰, P. T. Ge⁷⁶, Z. W. Ge⁴², C. Geng⁵⁹, E. M. Gersabeck⁶⁷, A. Gilman⁶⁹, K. Goetzen¹³, L. Gong⁴⁰, W. X. Gong^{1,58}, W. Gradi³⁵, S. Gramigna^{29A,29B}, M. Greco^{74A,74C}, M. H. Gu^{1,58}, Y. T. Gu¹⁵, C. Y. Guan^{1,63}, Z. L. Guan²², A. Q. Guo^{31,63}, L. B. Guo⁴¹, M. J. Guo⁵⁰, R. P. Guo⁴⁹, Y. P. Guo^{12,g}, A. Guskov^{36,b}, J. Gutierrez²⁷, K. L. Han⁶³, T. T. Han¹, X. Q. Hao¹⁹, F. A. Harris⁶⁵, K. K. He⁵⁵, K. L. He^{1,63}, F. H. Heinsius³, C. H. Heinz³⁵, Y. K. Heng^{1,58,63}, C. Herold⁶⁰, T. Holtmann³, P. C. Hong³⁴, G. Y. Hou^{1,63}, X. T. Hou^{1,63}, Y. R. Hou⁶³, Z. L. Hou¹, B. Y. Hu⁵⁹, H. M. Hu^{1,63}, J. F. Hu^{56,j}, S. L. Hu^{12,g}, T. Hu^{1,58,63}, Y. Hu¹, G. S. Huang^{71,58}, K. X. Huang⁵⁹, L. Q. Huang^{31,63}, X. T. Huang⁵⁰, Y. P. Huang¹, T. Hussain⁷³, F. Hölzken³, N. Hüskens^{27,35}, N. in der Wiesche⁶⁸, J. Jackson²⁷, S. Janchiv³², J. H. Jeong^{10A}, Q. Ji¹, Q. P. Ji¹⁹, W. Ji^{1,63}, X. B. Ji^{1,63}, X. L. Ji^{1,58}, Y. Y. Ji⁵⁰, X. Q. Jia⁵⁰, Z. K. Jia^{71,58}, D. Jiang^{1,63}, H. B. Jiang⁷⁶, P. C. Jiang^{46,h}, S. S. Jiang³⁹, T. J. Jiang¹⁶, X. S. Jiang^{1,58,63}, Y. Jiang⁶³, J. B. Jiao⁵⁰, J. K. Jiao³⁴, Z. Jiao²³, S. Jin⁴², Y. Jin⁶⁶, M. Q. Jing^{1,63}, X. M. Jing⁶³, T. Johansson⁷⁵, S. Kabana³³, N. Kalantar-Nayestanaki⁶⁴, X. L. Kang⁹, X. S. Kang⁴⁰, M. Kavatsyuk⁶⁴, B. C. Ke⁸⁰, V. Khachatryan²⁷, A. Khoukaz⁶⁸, R. Kiuchi¹, O. B. Kolcu^{62A}, B. Kopf³, M. Kuessner³, X. Kui^{1,63}, N. Kumar²⁶, A. Kupsc^{44,75}, W. Kühn³⁷, J. J. Lane⁶⁷, P. Larini¹⁸, L. Lavezzi^{74A,74C}, T. T. Lei^{71,58}, Z. H. Lei^{71,58}, M. Lellmann³⁵, T. Lenz³⁵, C. Li⁴⁷, C. Li⁴³, C. H. Li³⁹, Cheng Li^{71,58}, D. M. Li⁸⁰, F. Li^{1,58}, G. Li¹, H. B. Li^{1,63}, H. J. Li¹⁹, H. N. Li^{56,j}, Hui Li⁴³, J. R. Li⁶¹, J. S. Li⁵⁹, Ke Li¹, L. J. Li^{1,63}, L. K. Li¹, Lei Li⁴⁸, M. H. Li⁴³, P. R. Li^{38,l}, Q. M. Li^{1,63}, Q. X. Li⁵⁰, R. Li^{17,31}, S. X. Li¹², T. Li⁵⁰, W. D. Li^{1,63}, W. G. Li^{1,a}, X. Li^{1,63}, X. H. Li^{71,58}, X. L. Li⁵⁰, X. Z. Li⁵⁹, Xiaoyu Li^{1,63}, Y. G. Li^{46,h}, Z. J. Li⁵⁹, Z. X. Li¹⁵, C. Liang⁴², H. Liang^{71,58}, H. Liang^{1,63}, Y. F. Liang⁵⁴, Y. T. Liang^{31,63}, G. R. Liao¹⁴, L. Z. Liao⁵⁰, J. Libby²⁶, A. Limphirat⁶⁰, C. C. Lin⁵⁵, D. X. Lin^{31,63}, T. Lin¹, B. J. Liu¹, B. X. Liu⁷⁶, C. Liu³⁴, C. X. Liu¹, F. H. Liu⁵³, Fang Liu¹, Feng Liu⁶, G. M. Liu^{56,j}, H. Liu^{38,k,l}, H. B. Liu¹⁵, H. M. Liu^{1,63}, Huanhuan Liu¹, Huihui Liu²¹, J. B. Liu^{71,58}, J. Y. Liu^{1,63}, K. Liu^{38,k,l}, K. Y. Liu⁴⁰, Ke Liu²², L. Liu^{71,58}, L. C. Liu⁴³, Lu Liu⁴³, M. H. Liu^{12,g}, P. L. Liu¹, Q. Liu⁶³, S. B. Liu^{71,58}, T. Liu^{12,g}, W. K. Liu⁴³, W. M. Liu^{71,58}, X. Liu³⁹, X. Liu^{38,k,l}, Y. Liu⁸⁰, Y. Liu^{38,k,l}, Y. B. Liu⁴³, Z. A. Liu^{1,58,63}, Z. D. Liu⁹, Z. Q. Liu⁵⁰, X. C. Lou^{1,58,63}, F. X. Lu⁵⁹, H. J. Lu²³, J. G. Lu^{1,58}, X. L. Lu¹, Y. Lu⁷, Y. P. Lu^{1,58}, Z. H. Lu^{1,63}, C. L. Luo⁴¹, M. X. Luo⁷⁹, T. Luo^{12,g}, X. L. Luo^{1,58}, X. R. Lyu⁶³, Y. F. Lyu⁴³, F. C. Ma⁴⁰, H. Ma⁷⁸, H. L. Ma¹, J. L. Ma^{1,63}, L. L. Ma⁵⁰, M. M. Ma^{1,63}, Q. M. Ma¹, R. Q. Ma^{1,63}, T. Ma^{71,58}, X. T. Ma^{1,63}, X. Y. Ma^{1,58}, Y. Ma^{46,h}, Y. M. Ma³¹, F. E. Maas¹⁸, M. Maggiore^{74A,74C}, S. Malde⁶⁹, Y. J. Mao^{46,h}, Z. P. Mao¹, S. Marcello^{74A,74C}, Z. X. Meng⁶⁶, J. G. Messchendorp^{13,64}, G. Mezzadri^{29A}, H. Miao^{1,63}, T. J. Min⁴², R. E. Mitchell²⁷, X. H. Mo^{1,58,63}, B. Moses²⁷, N. Yu. Muchnoi^{4,c}, J. Muskalla³⁵, Y. Nefedov³⁶, F. Nerling^{18,e}, L. S. Nie²⁰, I. B. Nikolaev^{4,c}, Z. Ning^{1,58}, S. Nisar^{11,m}, Q. L. Niu^{38,k,l}, W. D. Niu⁵⁵, Y. Niu⁵⁰, S. L. Olsen⁶³, Q. Ouyang^{1,58,63}, S. Pacetti^{28B,28C}, X. Pan⁵⁵, Y. Pan⁵⁷, A. Pathak³⁴, P. Patteri^{28A}, Y. P. Pei^{71,58}, M. Pelizaeus³, H. P. Peng^{71,58}, Y. Y. Peng^{38,k,l}, K. Peters^{13,e}, J. L. Ping⁴¹, R. G. Ping^{1,63}, S. Plura³⁵, V. Prasad³³, F. Z. Qi¹, H. Qi^{71,58}, H. R. Qi⁶¹, M. Qi⁴², T. Y. Qi^{12,g}, S. Qian^{1,58}, W. B. Qian⁶³, C. F. Qiao⁶³, X. K. Qiao⁸⁰, J. J. Qin⁷², L. Q. Qin¹⁴, L. Y. Qin^{71,58}, X. S. Qin⁵⁰, Z. H. Qin^{1,58}, J. F. Qiu¹, Z. H. Qu⁷², C. F. Redmer³⁵, K. J. Ren³⁹, A. Rivetti^{74C}, M. Rolo^{74C}, G. Rong^{1,63}, Ch. Rosner¹⁸, S. N. Ruan⁴³, N. Salone⁴⁴, A. Sarantsev^{36,d}, Y. Schelhaas³⁵, K. Schoenning⁷⁵, M. Scodellaggio^{29A}, K. Y. Shan^{12,g}, W. Shan²⁴, X. Y. Shan^{71,58}, Z. J. Shang^{38,k,l}, J. F. Shangguan⁵⁵, L. G. Shao^{1,63}, M. Shao^{71,58}, C. P. Shen^{12,g}, H. F. Shen^{1,8}, W. H. Shen⁶³, X. Y. Shen^{1,63}, B. A. Shi⁶³, H. Shi^{71,58}, H. C. Shi^{71,58}, J. L. Shi^{12,g}, J. Y. Shi¹, Q. O. Shi⁵⁵, S. Y. Shi⁷², X. Shi^{1,58}, J. J. Song¹⁹, T. Z. Song⁵⁹, W. M. Song^{34,i}, Y. J. Song^{12,g}, Y. X. Song^{46,h,n}, S. Sosio^{74A,74C}, S. Spataro^{74A,74C}, F. Stieler³⁵, Y. J. Su⁶³, G. B. Sun⁷⁶, G. X. Sun¹, H. Sun⁶³, H. K. Sun¹, J. F. Sun¹⁹, K. Sun⁶¹, L. Sun⁷⁶, S. S. Sun^{1,63}, T. Sun^{51,f}, W. Y. Sun³⁴, Y. Sun⁹, Y. J. Sun^{71,58}, Y. Z. Sun¹, Z. Q. Sun^{1,63}, Z. T. Sun⁵⁰, C. J. Tang⁵⁴, G. Y. Tang¹, J. Tang⁵⁹, M. Tang^{71,58}, Y. A. Tang⁷⁶, L. Y. Tao⁷², Q. T. Tao^{25,i}, M. Tat⁶⁹, J. X. Teng^{71,58}, V. Thoren⁷⁵, W. H. Tian⁵⁹, Y. Tian^{31,63}, Z. F. Tian⁷⁶, I. Uman^{62B}, Y. Wan⁵⁵, S. J. Wang⁵⁰, B. Wang¹, B. L. Wang⁶³, Bo Wang^{71,58}, D. Y. Wang^{46,h}, F. Wang⁷², H. J. Wang^{38,k,l}, J. J. Wang⁷⁶, J. P. Wang⁵⁰, K. Wang^{1,58}, L. L. Wang¹, M. Wang⁵⁰, Meng Wang⁶³, N. Y. Wang⁶³, S. Wang^{38,k,l}, S. Wang^{12,g}, T. Wang^{12,g}, T. J. Wang⁴³, W. Wang⁵⁹, W. Wang⁷², W. P. Wang^{35,71,o}, X. Wang^{46,h}, X. F. Wang^{38,k,l}, X. J. Wang³⁹, X. L. Wang^{12,g}, X. N. Wang¹, Y. Wang⁶¹, Y. D. Wang⁴⁵, Y. F. Wang^{1,58,63}, Y. L. Wang¹⁹, Y. N. Wang⁴⁵, Y. Q. Wang¹, Yaqian Wang¹⁷, Yi Wang⁶¹, Z. Wang^{1,58}, Z. L. Wang⁷², Z. Y. Wang^{1,63}, Ziyi Wang⁶³, D. H. Wei¹⁴, F. Weidner⁶⁸, S. P. Wen¹, Y. R. Wen³⁹, U. Wiedner³, G. Wilkinson⁶⁹, M. Wolke⁷⁵, L. Wollenberg³, C. Wu³⁹, J. F. Wu^{1,8}, L. H. Wu¹, L. J. Wu^{1,63}, X. Wu^{12,g}, X. H. Wu³⁴, Y. Wu^{71,58}, Y. H. Wu⁵⁵, Y. J. Wu³¹, Z. Wu^{1,58}, L. Xia^{71,58}, X. M. Xian³⁹, B. H. Xiang^{1,63}, T. Xiang^{46,h}, D. Xiao^{38,k,l}, G. Y. Xiao⁴², S. Y. Xiao¹, Y. L. Xiao^{12,g}, Z. J. Xiao⁴¹, C. Xie⁴², X. H. Xie^{46,h}, Y. Xie⁵⁰, Y. G. Xie^{1,58}, Y. H. Xie⁶, Z. P. Xie^{71,58}, T. Y. Xing^{1,63}, C. F. Xu^{1,63}, C. J. Xu⁵⁹, G. F. Xu¹, H. Y. Xu⁶⁶,

M. Xu^{71,58}, Q. J. Xu¹⁶, Q. N. Xu³⁰, W. Xu¹, W. L. Xu⁶⁶, X. P. Xu⁵⁵, Y. C. Xu⁷⁷, Z. P. Xu⁴², Z. S. Xu⁶³, F. Yan^{12,g}, L. Yan^{12,g}, W. B. Yan^{71,58}, W. C. Yan⁸⁰, X. Q. Yan¹, H. J. Yang^{51,f}, H. L. Yang³⁴, H. X. Yang¹, Tao Yang¹, Y. Yang^{12,g}, Y. F. Yang⁴³, Y. X. Yang^{1,63}, Yifan Yang^{1,63}, Z. W. Yang^{38,k,l}, Z. P. Yao⁵⁰, M. Ye^{1,58}, M. H. Ye⁸, J. H. Yin¹, Z. Y. You⁵⁹, B. X. Yu^{1,58,63}, C. X. Yu⁴³, G. Yu^{1,63}, J. S. Yu^{25,i}, T. Yu⁷², X. D. Yu^{46,h}, Y. C. Yu⁸⁰, C. Z. Yuan^{1,63}, J. Yuan³⁴, L. Yuan², S. C. Yuan¹, Y. Yuan^{1,63}, Y. J. Yuan⁴⁵, Z. Y. Yuan⁵⁹, C. X. Yue³⁹, A. A. Zafar⁷³, F. R. Zeng⁵⁰, S. H. Zeng⁷², X. Zeng^{12,g}, Y. Zeng^{25,i}, Y. J. Zeng⁵⁹, X. Y. Zhai³⁴, Y. C. Zhai⁵⁰, Y. H. Zhan⁵⁹, A. Q. Zhang^{1,63}, B. L. Zhang^{1,63}, B. X. Zhang¹, D. H. Zhang⁴³, G. Y. Zhang¹⁹, H. Zhang^{71,58}, H. Zhang⁸⁰, H. C. Zhang^{1,58,63}, H. H. Zhang⁵⁹, H. H. Zhang³⁴, H. Q. Zhang^{1,58,63}, H. R. Zhang^{71,58}, H. Y. Zhang^{1,58}, J. Zhang⁵⁹, J. Zhang⁸⁰, J. J. Zhang⁵², J. L. Zhang²⁰, J. Q. Zhang⁴¹, J. S. Zhang^{12,g}, J. W. Zhang^{1,58,63}, J. X. Zhang^{38,k,l}, J. Y. Zhang¹, J. Z. Zhang^{1,63}, Jianyu Zhang⁶³, L. M. Zhang⁶¹, Lei Zhang⁴², P. Zhang^{1,63}, Q. Y. Zhang³⁴, R. Y. Zhang^{38,k,l}, Shuihan Zhang^{1,63}, Shulei Zhang^{25,i}, X. D. Zhang⁴⁵, X. M. Zhang¹, X. Y. Zhang⁵⁰, Y. Zhang⁷², Y. T. Zhang⁸⁰, Y. H. Zhang^{1,58}, Y. M. Zhang³⁹, Yan Zhang^{71,58}, Yao Zhang¹, Z. D. Zhang¹, Z. H. Zhang¹, Z. L. Zhang³⁴, Z. Y. Zhang⁴³, Z. Y. Zhang⁷⁶, Z. Z. Zhang⁴⁵, G. Zhao¹, J. Y. Zhao^{1,63}, J. Z. Zhao^{1,58}, Lei Zhao^{71,58}, Ling Zhao¹, M. G. Zhao⁴³, N. Zhao⁷⁸, R. P. Zhao⁶³, S. J. Zhao⁸⁰, Y. B. Zhao^{1,58}, Y. X. Zhao^{31,63}, Z. G. Zhao^{71,58}, A. Zhemchugov^{36,b}, B. Zheng⁷², B. M. Zheng³⁴, J. P. Zheng^{1,58}, W. J. Zheng^{1,63}, Y. H. Zheng⁶³, B. Zhong⁴¹, X. Zhong⁵⁹, H. Zhou⁵⁰, J. Y. Zhou³⁴, L. P. Zhou^{1,63}, S. Zhou⁶, X. Zhou⁷⁶, X. K. Zhou⁶, X. R. Zhou^{71,58}, X. Y. Zhou³⁹, Y. Z. Zhou^{12,g}, J. Zhu⁴³, K. Zhu¹, K. J. Zhu^{1,58,63}, K. S. Zhu^{12,g}, L. Zhu³⁴, L. X. Zhu⁶³, S. H. Zhu⁷⁰, S. Q. Zhu⁴², T. J. Zhu^{12,g}, W. D. Zhu⁴¹, Y. C. Zhu^{71,58}, Z. A. Zhu^{1,63}, J. H. Zou¹, J. Zu^{71,58}

(BESIII Collaboration)

¹ Institute of High Energy Physics, Beijing 100049, People's Republic of China

² Beihang University, Beijing 100191, People's Republic of China

³ Bochum Ruhr-University, D-44780 Bochum, Germany

⁴ Budker Institute of Nuclear Physics SB RAS (BINP), Novosibirsk 630090, Russia

⁵ Carnegie Mellon University, Pittsburgh, Pennsylvania 15213, USA

⁶ Central China Normal University, Wuhan 430079, People's Republic of China

⁷ Central South University, Changsha 410083, People's Republic of China

⁸ China Center of Advanced Science and Technology, Beijing 100190, People's Republic of China

⁹ China University of Geosciences, Wuhan 430074, People's Republic of China

¹⁰ Chung-Ang University, Seoul, 06974, Republic of Korea

¹¹ COMSATS University Islamabad, Lahore Campus, Defence Road, Off Raiwind Road, 54000 Lahore, Pakistan

¹² Fudan University, Shanghai 200433, People's Republic of China

¹³ GSI Helmholtzcentre for Heavy Ion Research GmbH, D-64291 Darmstadt, Germany

¹⁴ Guangxi Normal University, Guilin 541004, People's Republic of China

¹⁵ Guangxi University, Nanning 530004, People's Republic of China

¹⁶ Hangzhou Normal University, Hangzhou 310036, People's Republic of China

¹⁷ Hebei University, Baoding 071002, People's Republic of China

¹⁸ Helmholtz Institute Mainz, Staudinger Weg 18, D-55099 Mainz, Germany

¹⁹ Henan Normal University, Xinxiang 453007, People's Republic of China

²⁰ Henan University, Kaifeng 475004, People's Republic of China

²¹ Henan University of Science and Technology, Luoyang 471003, People's Republic of China

²² Henan University of Technology, Zhengzhou 450001, People's Republic of China

²³ Huangshan College, Huangshan 245000, People's Republic of China

²⁴ Hunan Normal University, Changsha 410081, People's Republic of China

²⁵ Hunan University, Changsha 410082, People's Republic of China

²⁶ Indian Institute of Technology Madras, Chennai 600036, India

²⁷ Indiana University, Bloomington, Indiana 47405, USA

²⁸ INFN Laboratori Nazionali di Frascati, (A)INFN Laboratori Nazionali di Frascati, I-00044, Frascati, Italy; (B)INFN Sezione di Perugia, I-06100, Perugia, Italy; (C)University of Perugia, I-06100, Perugia, Italy

²⁹ INFN Sezione di Ferrara, (A)INFN Sezione di Ferrara, I-44122, Ferrara, Italy; (B)University of Ferrara, I-44122, Ferrara, Italy

³⁰ Inner Mongolia University, Hohhot 010021, People's Republic of China

³¹ Institute of Modern Physics, Lanzhou 730000, People's Republic of China

³² Institute of Physics and Technology, Peace Avenue 54B, Ulaanbaatar 13330, Mongolia

³³ Instituto de Alta Investigación, Universidad de Tarapacá, Casilla 7D, Arica 1000000, Chile

³⁴ Jilin University, Changchun 130012, People's Republic of China

³⁵ Johannes Gutenberg University of Mainz, Johann-Joachim-Becher-Weg 45, D-55099 Mainz, Germany

³⁶ Joint Institute for Nuclear Research, 141980 Dubna, Moscow region, Russia

³⁷ Justus-Liebig-Universitaet Giessen, II. Physikalisches Institut, Heinrich-Buff-Ring 16, D-35392 Giessen, Germany

³⁸ Lanzhou University, Lanzhou 730000, People's Republic of China

³⁹ Liaoning Normal University, Dalian 116029, People's Republic of China

⁴⁰ Liaoning University, Shenyang 110036, People's Republic of China

⁴¹ Nanjing Normal University, Nanjing 210023, People's Republic of China

⁴² Nanjing University, Nanjing 210093, People's Republic of China

- ⁴³ Nankai University, Tianjin 300071, People's Republic of China
⁴⁴ National Centre for Nuclear Research, Warsaw 02-093, Poland
⁴⁵ North China Electric Power University, Beijing 102206, People's Republic of China
⁴⁶ Peking University, Beijing 100871, People's Republic of China
⁴⁷ Qufu Normal University, Qufu 273165, People's Republic of China
⁴⁸ Renmin University of China, Beijing 100872, People's Republic of China
⁴⁹ Shandong Normal University, Jinan 250014, People's Republic of China
⁵⁰ Shandong University, Jinan 250100, People's Republic of China
⁵¹ Shanghai Jiao Tong University, Shanghai 200240, People's Republic of China
⁵² Shanxi Normal University, Linfen 041004, People's Republic of China
⁵³ Shanxi University, Taiyuan 030006, People's Republic of China
⁵⁴ Sichuan University, Chengdu 610064, People's Republic of China
⁵⁵ Soochow University, Suzhou 215006, People's Republic of China
⁵⁶ South China Normal University, Guangzhou 510006, People's Republic of China
⁵⁷ Southeast University, Nanjing 211100, People's Republic of China
⁵⁸ State Key Laboratory of Particle Detection and Electronics, Beijing 100049, Hefei 230026, People's Republic of China
⁵⁹ Sun Yat-Sen University, Guangzhou 510275, People's Republic of China
⁶⁰ Suranaree University of Technology, University Avenue 111, Nakhon Ratchasima 30000, Thailand
⁶¹ Tsinghua University, Beijing 100084, People's Republic of China
⁶² Turkish Accelerator Center Particle Factory Group, (A)Istinye University, 34010, Istanbul, Turkey; (B)Near East University, Nicosia, North Cyprus, 99138, Mersin 10, Turkey
⁶³ University of Chinese Academy of Sciences, Beijing 100049, People's Republic of China
⁶⁴ University of Groningen, NL-9747 AA Groningen, The Netherlands
⁶⁵ University of Hawaii, Honolulu, Hawaii 96822, USA
⁶⁶ University of Jinan, Jinan 250022, People's Republic of China
⁶⁷ University of Manchester, Oxford Road, Manchester, M13 9PL, United Kingdom
⁶⁸ University of Muenster, Wilhelm-Klemm-Strasse 9, 48149 Muenster, Germany
⁶⁹ University of Oxford, Keble Road, Oxford OX13RH, United Kingdom
⁷⁰ University of Science and Technology Liaoning, Anshan 114051, People's Republic of China
⁷¹ University of Science and Technology of China, Hefei 230026, People's Republic of China
⁷² University of South China, Hengyang 421001, People's Republic of China
⁷³ University of the Punjab, Lahore-54590, Pakistan
⁷⁴ University of Turin and INFN, (A)University of Turin, I-10125, Turin, Italy; (B)University of Eastern Piedmont, I-15121, Alessandria, Italy; (C)INFN, I-10125, Turin, Italy
⁷⁵ Uppsala University, Box 516, SE-75120 Uppsala, Sweden
⁷⁶ Wuhan University, Wuhan 430072, People's Republic of China
⁷⁷ Yantai University, Yantai 264005, People's Republic of China
⁷⁸ Yunnan University, Kunming 650500, People's Republic of China
⁷⁹ Zhejiang University, Hangzhou 310027, People's Republic of China
⁸⁰ Zhengzhou University, Zhengzhou 450001, People's Republic of China
- ^a Deceased
- ^b Also at the Moscow Institute of Physics and Technology, Moscow 141700, Russia
^c Also at the Novosibirsk State University, Novosibirsk, 630090, Russia
^d Also at the NRC "Kurchatov Institute", PNPI, 188300, Gatchina, Russia
^e Also at Goethe University Frankfurt, 60323 Frankfurt am Main, Germany
- ^f Also at Key Laboratory for Particle Physics, Astrophysics and Cosmology, Ministry of Education; Shanghai Key Laboratory for Particle Physics and Cosmology; Institute of Nuclear and Particle Physics, Shanghai 200240, People's Republic of China
- ^g Also at Key Laboratory of Nuclear Physics and Ion-beam Application (MOE) and Institute of Modern Physics, Fudan University, Shanghai 200443, People's Republic of China
- ^h Also at State Key Laboratory of Nuclear Physics and Technology, Peking University, Beijing 100871, People's Republic of China
- ⁱ Also at School of Physics and Electronics, Hunan University, Changsha 410082, China
- ^j Also at Guangdong Provincial Key Laboratory of Nuclear Science, Institute of Quantum Matter, South China Normal University, Guangzhou 510006, China
- ^k Also at MOE Frontiers Science Center for Rare Isotopes, Lanzhou University, Lanzhou 730000, People's Republic of China
- ^l Also at Lanzhou Center for Theoretical Physics, Lanzhou University, Lanzhou 730000, People's Republic of China
- ^m Also at the Department of Mathematical Sciences, IBA, Karachi 75270, Pakistan
- ⁿ Also at Ecole Polytechnique Federale de Lausanne (EPFL), CH-1015 Lausanne, Switzerland
- ^o Also at Helmholtz Institute Mainz, Staudinger Weg 18, D-55099 Mainz, Germany

Using $(10.087 \pm 0.044) \times 10^9 J/\psi$ events collected with the BESIII detector at the BEPCII storage ring, the processes $\Lambda p \rightarrow \Lambda p$ and $\bar{\Lambda} p \rightarrow \bar{\Lambda} p$ are studied, where the $\Lambda/\bar{\Lambda}$ baryons are produced in the process $J/\psi \rightarrow \Lambda\bar{\Lambda}$ and the protons are the hydrogen nuclei in the cooling oil of the beam pipe. Clear signals are observed for the two reactions. The cross sections in $-0.9 \leq \cos\theta_{\Lambda/\bar{\Lambda}} \leq 0.9$ are measured to be $\sigma(\Lambda p \rightarrow \Lambda p) = (12.2 \pm 1.6_{\text{stat}} \pm 1.1_{\text{sys}})$ mb and $\sigma(\bar{\Lambda} p \rightarrow \bar{\Lambda} p) = (17.5 \pm 2.1_{\text{stat}} \pm 1.6_{\text{sys}})$ mb at the $\Lambda/\bar{\Lambda}$ momentum of $1.074 \text{ GeV}/c$ within a range of $\pm 0.017 \text{ GeV}/c$, where the $\theta_{\Lambda/\bar{\Lambda}}$ are the scattering angles of the $\Lambda/\bar{\Lambda}$ in the $\Lambda p/\bar{\Lambda} p$ rest frames. Furthermore, the differential cross sections of the two reactions are also measured, where there is a slight tendency of forward scattering for $\Lambda p \rightarrow \Lambda p$, and a strong forward peak for $\bar{\Lambda} p \rightarrow \bar{\Lambda} p$. We present an approach to extract the total elastic cross sections by extrapolation. The study of $\bar{\Lambda} p \rightarrow \bar{\Lambda} p$ represents the first study of antihyperon-nucleon scattering, and these new measurements will serve as important inputs for the theoretical understanding of the (anti)hyperon-nucleon interaction.

One of the main goals of nuclear physics is to understand baryon-baryon interaction in a unified perspective. To achieve this purpose, plentiful nucleon-nucleon (NN) and antinucleon-nucleon ($\bar{N}N$) scattering data have been measured [1]. Therefore, the relevant theory of NN and $\bar{N}N$ interactions is well established, and it can be tightly constrained by experimental data. However, the understanding of hyperon-nucleon (YN) interaction has a large uncertainty due to the lack of relevant measurements. The YN interaction is studied mainly via three methods. The first is to extract the YN correlation functions in heavy-ion collisions [2–5], the second is to study hypernuclei [6–9], and the third is to investigate YN scattering [10–12]. The last method is the most direct way to study YN interaction, but it is limited by the availability and short-lifetime of hyperon beams, leading to a scarcity of YN scattering data [1]. The study of YN interaction is also crucial to determine the equation of state (EoS) of nuclear matter at supersaturation densities and understand the so-called “hyperon puzzle” of neutron stars (NS) [13–18]. To solve these issues, more YN scattering data is desired to constrain the calculations of YN interaction.

Compared to the YN scattering, the situation is even worse for antihyperon-nucleon ($\bar{Y}N$) scattering. Until now, no $\bar{Y}N$ scattering data have been obtained due to the absence effective antihyperon sources [1], which results in the very limited related theoretical research. Therefore, the realization of $\bar{Y}N$ scattering measurements can fill this gap, and new measurements will motivate more effort for the understanding of the $\bar{Y}N$ interaction. More importantly, $\bar{Y}N$ scattering data can further constrain the YN interaction theory from another angle.

In this Letter, we present a study of the reactions $\Lambda p \rightarrow \Lambda p$ and $\bar{\Lambda} p \rightarrow \bar{\Lambda} p$, where Λ and $\bar{\Lambda}$ are reconstructed via the decays $\Lambda \rightarrow p\pi^-$ and $\bar{\Lambda} \rightarrow \bar{p}\pi^+$. The cross sections and differential cross sections of the two reactions are all measured. This is the first study of $\bar{Y}N$ scattering.

The BESIII detector records symmetric e^+e^- collisions at the BEPCII collider [19]. Details of the BESIII detector can be found in Ref. [20]. The material of the beam pipe is composed of gold (^{197}Au), beryllium (^9Be) and oil ($^{12}\text{C} : ^1\text{H} = 1 : 2.13$), as shown in Fig. 1. With a

sample of $(10.087 \pm 0.044) \times 10^9 J/\psi$ events collected by the BESIII detector [21], intense almost monoenergetic $\Lambda/\bar{\Lambda}$ hyperons with a momentum of $1.074 \text{ GeV}/c$ within a range of $\pm 0.017 \text{ GeV}/c$ can be produced via the decay $J/\psi \rightarrow \Lambda\bar{\Lambda}$, the momentum spread is due to the small horizontal crossing angle of $\pm 11 \text{ mrad}$ for e^\pm beams. Afterwards the $\Lambda/\bar{\Lambda}$ baryons can interact with the material in the beam pipe. A similar idea was proposed forty years ago using $\bar{p}p$ collisions at a LEAR experiment [22]. Especially, Ref. [23] has used this method to perform the first study of YN interaction using Ξ^0 -nucleus scattering at BESIII, and Λ -nucleus scattering was measured in Ref. [24]. Furthermore, utilizing the almost static protons in the ^1H of the cooling oil of the beam pipe, the information on the interaction between (anti)hyperon and proton can be directly extracted via (anti)hyperon-proton scattering in this way.

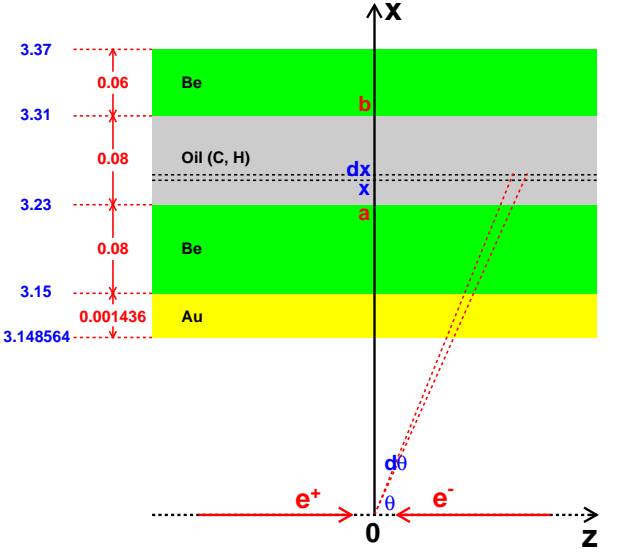


FIG. 1. Schematic diagram of the beam pipe, the length units are centimeter (cm). The z -axis is the symmetry axis of the MDC, and the x -axis is perpendicular to the e^+e^- beam direction.

In this analysis, simulated data samples are produced

with a GEANT4-based [25] Monte Carlo (MC) package, which includes the geometric description of the BESIII detector [20] and the detector response. They are used to determine detection efficiencies and to estimate backgrounds. The simulation models the beam energy spread and initial state radiation (ISR) in the e^+e^- annihilations with the generator KKMC [26]. The inclusive MC sample includes both the production of the J/ψ resonance and the continuum processes incorporated in KKMC [26]. All particle decays are modeled with EVTGEN [27] using branching fractions either taken from the Particle Data Group (PDG) [1], where available, or otherwise estimated with LUNDCHARM [28]. Final state radiation (FSR) from charged final state particles is incorporated using the PHOTOS package [29]. The signal process considered in this analysis is $J/\psi \rightarrow \Lambda\bar{\Lambda}$ with either $\Lambda p \rightarrow \Lambda p$ or $\bar{\Lambda}p \rightarrow \bar{\Lambda}p$, $\Lambda \rightarrow p\pi^-$, $\bar{\Lambda} \rightarrow \bar{p}\pi^+$. In the signal simulation, the angular distribution of $J/\psi \rightarrow \Lambda\bar{\Lambda}$ is generated according to the measurement in Ref. [30]. We simulate the reactions $\Lambda p \rightarrow \Lambda p/\bar{\Lambda}p \rightarrow \bar{\Lambda}p$ by taking the proton to be at rest, and the hyperon angular distribution is generated using an isotropic phase-space distribution to obtain the angle dependent detection efficiency.

Charged tracks detected in the multilayer drift chamber (MDC) are required to be within a polar angle (θ) range of $|\cos\theta| < 0.93$, where θ is the angle between the charged track and the z -axis, which is the symmetry axis of the MDC. Particle identification for charged tracks combines measurements of the energy loss (dE/dx) in the MDC and the flight time in the time-of-flight system (TOF) to form likelihoods $\mathcal{L}(h)$ ($h = p, K, \pi$) for each hadron h hypothesis. Tracks are identified as protons when the proton hypothesis has the greatest likelihood ($\mathcal{L}(p) > \mathcal{L}(\pi)$ and $\mathcal{L}(p) > \mathcal{L}(K)$), while charged pions are identified by comparing the likelihoods for the pion hypotheses, ($\mathcal{L}(\pi) > \mathcal{L}(K)$ and $\mathcal{L}(\pi) > \mathcal{L}(p)$).

Since the final states of the two reactions all contain $p\bar{p}\pi^+\pi^-$, candidate events must have five charged tracks, and two p , one \bar{p} , one π^+ and one π^- are required to be identified. For the decay $\bar{\Lambda} \rightarrow \bar{p}\pi^+$, we perform a vertex fit to the $\bar{p}\pi^+$ combination, and the $\bar{\Lambda}$ signal region is defined as $|M(\bar{p}\pi^+) - m_{\bar{\Lambda}}| < 0.003 \text{ GeV}/c^2$, where $m_{\bar{\Lambda}}$ is the nominal mass of the $\bar{\Lambda}$. In this Letter, all nominal masses are taken from PDG [1]. For the decay $\Lambda \rightarrow p\pi^-$, we perform the vertex fit by considering both $p\pi^-$ combinations. The $p\pi^-$ combination with the smallest value of $|M(p\pi^-) - m_{\Lambda}|$, where m_{Λ} is the Λ nominal mass, is taken as Λ candidate. The Λ signal region is defined as $|M(p\pi^-) - m_{\Lambda}| < 0.003 \text{ GeV}/c^2$. Finally, a vertex fit is performed to the combination of the $\Lambda/\bar{\Lambda}$ and the remaining p for the reactions $\Lambda p \rightarrow \Lambda p/\bar{\Lambda}p \rightarrow \bar{\Lambda}p$.

To select the signal events of $J/\psi \rightarrow \Lambda\bar{\Lambda}$, the invariant mass recoiling against the $\Lambda/\bar{\Lambda}$, $M_{\text{recoil}}(\bar{\Lambda}/\Lambda)$, is required to be in the $\Lambda/\bar{\Lambda}$ signal region, defined as $[m_{\Lambda/\bar{\Lambda}} - 0.020, m_{\Lambda/\bar{\Lambda}} + 0.016] \text{ GeV}/c^2$, where $M_{\text{recoil}}(\bar{\Lambda}/\Lambda) \equiv$

$\sqrt{E_{\text{beam}}^2 - |\vec{p}_{\bar{\Lambda}/\Lambda} c|^2/c^2}$, E_{beam} is the e^\pm beam energy, and $\vec{p}_{\bar{\Lambda}/\Lambda}$ is the measured momentum of the $\bar{\Lambda}/\Lambda$ candidate in the e^+e^- rest frame. The main background is $J/\psi \rightarrow \Lambda\bar{\Lambda}$, $\Lambda \rightarrow p\pi^-$, $\bar{\Lambda} \rightarrow \bar{p}\pi^+$, where no scattering of $\Lambda/\bar{\Lambda}$ with a proton from the beam pipe occurred. To suppress this background, the recoil mass of $\bar{\Lambda}p_{\Lambda}/\bar{\Lambda}\bar{p}$, $M_{\text{recoil}}(\bar{\Lambda}p_{\Lambda}/\bar{\Lambda}\bar{p})$, is obtained from the four-momenta of the initial e^+e^- system and the $\bar{\Lambda}/\Lambda$ and p_{Λ}/\bar{p} candidates, where p_{Λ} is the proton from Λ decays. $M_{\text{recoil}}(\bar{\Lambda}p_{\Lambda}/\bar{\Lambda}\bar{p})$ should be around the nominal π^-/π^+ mass for this background, so we require $M_{\text{recoil}}(\bar{\Lambda}p_{\Lambda}/\bar{\Lambda}\bar{p}) < 0 \text{ GeV}/c^2$ to remove these events. To select those signal events that react with the cooling oil in the beam pipe, the R_{xy} signal region is defined as $[3.0, 3.5] \text{ cm}$, taking into account the detector resolution, where R_{xy} is the distance from the reconstructed $\Lambda p/\bar{\Lambda}p$ vertex to the z -axis. To remove the events from the reactions between $\Lambda/\bar{\Lambda}$ and $^{197}\text{Au}/^{9}\text{Be}/^{12}\text{C}$ nuclei, we define the momentum of the proton in the ^1H of the cooling oil as $P(p_{\text{oil}}) \equiv |\vec{P}_{\Lambda/\bar{\Lambda}} + \vec{P}_p - (\vec{P}_{e^+e^-} - \vec{P}_{\Lambda/\bar{\Lambda}})|$, where \vec{P} represents the momentum of each particle in the lab frame. Because the proton in the ^1H of the cooling oil is practically static, while the proton in the $^{197}\text{Au}/^{9}\text{Be}/^{12}\text{C}$ nuclei has Fermi momentum, the $P(p_{\text{oil}})$ should be around zero for signal processes but hundreds of MeV/c for background processes. To remove these events, the requirement $P(p_{\text{oil}}) < 0.04 \text{ GeV}/c$ is applied.

For the signal reactions $\Lambda p \rightarrow \Lambda p$ and $\bar{\Lambda}p \rightarrow \bar{\Lambda}p$ produced from the decay $J/\psi \rightarrow \Lambda\bar{\Lambda}$, the center-of-mass energies for the incident $\Lambda/\bar{\Lambda}$ and a static p are all $2.243 \text{ GeV}/c^2$ within a range of $\pm 0.005 \text{ GeV}/c^2$. Figure 2 shows the $M(\Lambda p)$ and $M(\bar{\Lambda}p)$ distributions from data after the final event selection. Clear enhancements are seen around $2.243 \text{ GeV}/c^2$, corresponding to the reactions $\Lambda p \rightarrow \Lambda p$ and $\bar{\Lambda}p \rightarrow \bar{\Lambda}p$, respectively. A detailed study of the J/ψ inclusive MC sample shows that there is no peaking background in the signal region. To determine the signal yield, an unbinned maximum likelihood fit is performed to the $M(\Lambda p)$ distribution and $M(\bar{\Lambda}p)$ distribution, respectively. We use the MC-determined shape convolved with a free Gaussian function to describe the signal, where the yield acts as a free fit parameter. The free Gaussian function is used to describe the difference in the data and signal MC resolutions. The background is described by a uniform distribution with the number of events as free parameter. The fit results are shown in Fig. 2. The signal yields returned by the fits are $N_{\Lambda p}^{\text{sig}} = 60.9 \pm 7.8$ and $N_{\bar{\Lambda}p}^{\text{sig}} = 72.0 \pm 8.5$ for the reactions $\Lambda p \rightarrow \Lambda p$ and $\bar{\Lambda}p \rightarrow \bar{\Lambda}p$, respectively, and the goodness of the fits for the two reactions are $\chi^2/\text{ndf} = 4.8/4 = 1.2$ and $0.8/4 = 0.2$ without considering empty bins.

To extract the differential cross sections for the two reactions, we need the signal yields as a function of $\cos\theta_{\Lambda/\bar{\Lambda}}$, where $\theta_{\Lambda/\bar{\Lambda}}$ is the scattering angle of the scattered $\Lambda/\bar{\Lambda}$ in the $\Lambda p/\bar{\Lambda}p$ rest frames with the z -axis defined by the

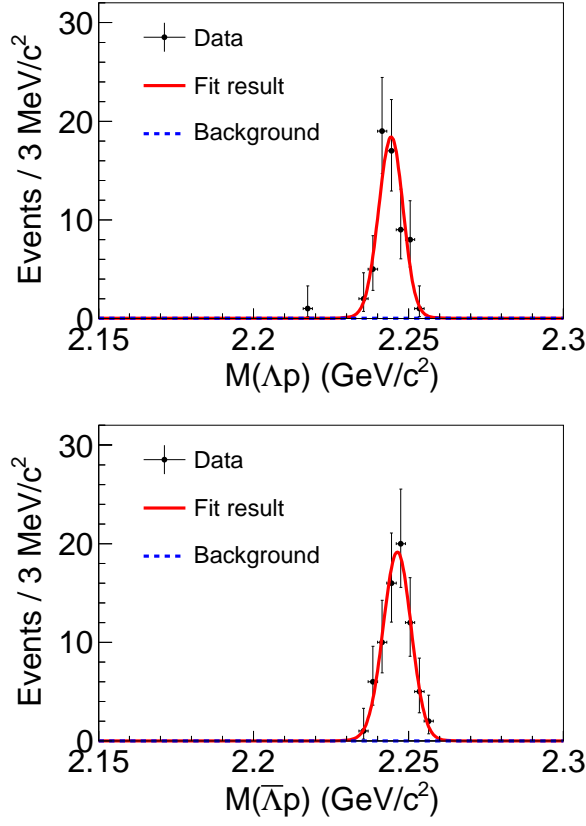


FIG. 2. Distributions of $M(\Lambda p)$ (top) and $M(\bar{\Lambda} p)$ (bottom) of data (black dots with error bars) for the reactions $\Lambda p \rightarrow \Lambda p$ and $\bar{\Lambda} p \rightarrow \bar{\Lambda} p$, respectively. The red solid curve is the total fit result and the blue dashed curve is the background component.

incident $\Lambda/\bar{\Lambda}$ momentum. Because the efficiency is very low and it is hard to obtain accurate experimental information near the regions $\cos\theta_{\Lambda/\bar{\Lambda}} = \pm 1$ due to the low momentum of scattered $\Lambda/\bar{\Lambda}$ or p , the measurements are restricted to $-0.9 \leq \cos\theta_{\Lambda/\bar{\Lambda}} \leq 0.9$. To obtain the number of signal events, we perform a simultaneous fit to the $M(\Lambda p)$ and $M(\bar{\Lambda} p)$ distributions in nine different $\cos\theta_{\Lambda/\bar{\Lambda}}$ regions, where the signal shape and background shape are the same as mentioned above. The obtained number of signal events in the nine $\cos\theta_{\Lambda/\bar{\Lambda}}$ regions are summarized in Table I. It is worth mentioning that no events survived in the $-1.0 < \cos\theta_{\Lambda/\bar{\Lambda}} < -0.9$ and the $0.9 < \cos\theta_{\Lambda/\bar{\Lambda}} < 1.0$ regions for data.

Using the same method as in Ref. [23], the cross sections of the reactions $\Lambda p \rightarrow \Lambda p$ and $\bar{\Lambda} p \rightarrow \bar{\Lambda} p$ can be determined, the only difference is that we use the proton in the 1H of the cooling oil of the beam pipe as the target material. The total elastic cross sections are calculated

TABLE I. Relevant parameters for the differential cross sections, where $\cos\theta_{\Lambda/\bar{\Lambda}}$ is the scattering angle, N_i^{sig} is the number of signal events, ϵ_i is the efficiency, $\frac{d\sigma}{d\Omega}$ is the differential cross section, and i represents the different $\cos\theta_{\Lambda/\bar{\Lambda}}$ bins. The first value in parentheses is for $\Lambda p \rightarrow \Lambda p$, and the second for $\bar{\Lambda} p \rightarrow \bar{\Lambda} p$.

$\cos\theta_{\Lambda/\bar{\Lambda}}$	N_i^{sig}	ϵ_i (%)	$\frac{d\sigma}{d\Omega}$ (mb/sr)
$[-0.9, -0.7]$	$(5.0^{+2.6}_{-1.9}, 0.0^{+1.1}_{-0.0})$	$(6.94, 4.93)$	$(1.7^{+0.9}_{-0.7}, 0.0^{+0.5}_{-0.0})$
$(-0.7, -0.5]$	$(1.0^{+1.4}_{-0.7}, 0.0^{+1.1}_{-0.0})$	$(14.13, 10.44)$	$(0.2^{+0.2}_{-0.1}, 0.0^{+0.3}_{-0.0})$
$(-0.5, -0.3]$	$(1.0^{+1.4}_{-0.7}, 1.0^{+1.4}_{-0.7})$	$(17.32, 13.27)$	$(0.2^{+0.2}_{-0.1}, 0.2^{+0.3}_{-0.1})$
$(-0.3, -0.1]$	$(11.0^{+3.7}_{-3.0}, 0.0^{+1.1}_{-0.0})$	$(17.74, 14.66)$	$(1.5^{+0.5}_{-0.4}, 0.0^{+0.2}_{-0.0})$
$(-0.1, 0.1]$	$(6.9^{+3.0}_{-2.3}, 0.0^{+1.1}_{-0.0})$	$(19.11, 15.79)$	$(0.9^{+0.4}_{-0.3}, 0.0^{+0.0}_{-0.0})$
$(0.1, 0.3]$	$(5.0^{+2.6}_{-1.9}, 2.0^{+1.8}_{-1.1})$	$(19.53, 16.82)$	$(0.6^{+0.3}_{-0.2}, 0.3^{+0.3}_{-0.2})$
$(0.3, 0.5]$	$(12.0^{+3.8}_{-3.1}, 7.0^{+3.0}_{-2.3})$	$(19.21, 17.68)$	$(1.5^{+0.5}_{-0.4}, 1.0^{+0.4}_{-0.3})$
$(0.5, 0.7]$	$(13.0^{+3.9}_{-3.3}, 25.0^{+5.3}_{-4.7})$	$(19.71, 17.60)$	$(1.6^{+0.5}_{-0.4}, 3.4^{+0.7}_{-0.6})$
$(0.7, 0.9]$	$(6.0^{+2.8}_{-2.1}, 37.0^{+6.4}_{-5.8})$	$(9.80, 9.93)$	$(1.5^{+0.7}_{-0.5}, 9.0^{+1.6}_{-1.4})$

with

$$\sigma(\Lambda p \rightarrow \Lambda p / \bar{\Lambda} p \rightarrow \bar{\Lambda} p) = \frac{N_{\Lambda p / \bar{\Lambda} p}^{\text{sig}}}{\epsilon_{\Lambda p / \bar{\Lambda} p} \mathcal{B} \mathcal{L}_{\text{eff}}}, \quad (1)$$

where $\epsilon_{\Lambda p / \bar{\Lambda} p} = \frac{\sum_i \epsilon_i (\frac{d\sigma}{d\Omega})_i}{\sum_i (\frac{d\sigma}{d\Omega})_i}$ is the weighted selection efficiency according to the differential cross section distribution, which will be introduced later. \mathcal{B} is the product of the branching ratios of the intermediate states, defined as $\mathcal{B} \equiv \mathcal{B}(\Lambda \rightarrow p\pi^-)\mathcal{B}(\bar{\Lambda} \rightarrow \bar{p}\pi^+)$, and \mathcal{L}_{eff} is the effective luminosity of the reaction of the $\Lambda/\bar{\Lambda}$ flux produced from $J/\psi \rightarrow \Lambda\bar{\Lambda}$ with the target material:

$$\mathcal{L}_{\text{eff}} = \frac{N_{J/\psi} \mathcal{B}_{J/\psi}}{2 + \frac{2}{3}\alpha} \int_a^b \int_0^\pi (1 + \alpha \cos^2 \theta) e^{-\frac{x}{\sin\theta \beta \gamma L}} N_H d\theta dx. \quad (2)$$

In the integral of this formula, the angular distribution of the $\Lambda/\bar{\Lambda}$ flux, the attenuation of the $\Lambda/\bar{\Lambda}$ flux and the number of target nuclei are considered. $N_{J/\psi}$ is the number of J/ψ events, $\mathcal{B}_{J/\psi}$ is the branching fraction of $J/\psi \rightarrow \Lambda\bar{\Lambda}$, and α is the parameter of the angular distribution of $J/\psi \rightarrow \Lambda\bar{\Lambda}$, $\beta\gamma \equiv \frac{\sqrt{E_{\text{beam}}^2 - m_{\Lambda/\bar{\Lambda}}^2 c^4}}{m_{\Lambda/\bar{\Lambda}} c^2}$ is the ratio of the momentum to the mass of the $\Lambda/\bar{\Lambda}$, and $L \equiv ct$ is the product of the speed of light and the mean lifetime of the $\Lambda/\bar{\Lambda}$ [1]. N_H is the number of target nuclei per unit volume, a and b are the distances from the inner surface and outer surface of the cooling oil in the beam pipe to the z -axis, θ and x are the angle and distance to the z -axis, as shown in Fig. 1. The beam pipe can be regarded as infinitely long with respect to the product of $\beta\gamma L$ for $\Lambda/\bar{\Lambda}$. The parameters are listed in Table II, and the corresponding total elastic cross sections in $-0.9 \leq \cos\theta_{\Lambda/\bar{\Lambda}} \leq 0.9$ are measured to be $\sigma(\Lambda p \rightarrow \Lambda p) = (12.2 \pm 1.6_{\text{stat}} \pm 1.1_{\text{sys}})$ mb and $\sigma(\bar{\Lambda} p \rightarrow \bar{\Lambda} p) = (17.5 \pm 2.1_{\text{stat}} \pm 1.4_{\text{sys}})$ mb.

1.6_{sys}) mb at a $\Lambda/\bar{\Lambda}$ momentum of 1.074 GeV/ c within a range of ± 0.017 GeV/ c .

TABLE II. Input parameters for the cross section calculations. The first value in brackets is for $\Lambda p \rightarrow \Lambda p$, and the second is for $\bar{\Lambda} p \rightarrow \bar{\Lambda} p$.

Parameter	Result
$N_{\Lambda p/\bar{\Lambda} p}^{\text{sig}}$	$(60.9 \pm 7.8, 72.0 \pm 8.5)$
$\epsilon_{\Lambda p/\bar{\Lambda} p}$	$(15.29\%, 12.55\%)$
\mathcal{B}	$(40.8321 \pm 0.4518)\%$ [1]
$N_{J/\psi}$	$(10.087 \pm 0.044) \times 10^9$ [21]
$\mathcal{B}_{J/\psi}$	$(0.189 \pm 0.009)\%$ [1]
α	0.475 ± 0.004 [30]
L	(7.89 ± 0.06) cm [1]
E_{beam}	1.5485 GeV
$m_{\Lambda/\bar{\Lambda}}$	(1.115683 ± 0.000006) GeV/ c^2 [1]
a	3.23 cm [20]
b	3.31 cm [20]
N_H	7.35×10^{22} cm $^{-3}$

The differential cross sections for the reactions $\Lambda p \rightarrow \Lambda p$ and $\bar{\Lambda} p \rightarrow \bar{\Lambda} p$ are calculated with

$$\left(\frac{d\sigma}{d\Omega}\right)_i = \frac{N_i^{\text{sig}}}{\epsilon_i \mathcal{B} \mathcal{L}_{\text{eff}} \Delta\Omega}, \quad (3)$$

where N_i^{sig} and ϵ_i are the number of signal events and efficiency, i represents different $\cos\theta_{\Lambda/\bar{\Lambda}}$ bins, and $\Delta\Omega = 2\pi\Delta\cos\theta_{\Lambda/\bar{\Lambda}} = 0.4\pi$ represents the solid angle. The measured results are listed in Table I and shown in Fig. 3. We can see there is a slight tendency of forward scattering for $\Lambda p \rightarrow \Lambda p$, while there is a strong forward peak for $\bar{\Lambda} p \rightarrow \bar{\Lambda} p$. The different behaviors indicate that the reaction mechanisms of these two processes are different.

We also tested an extrapolation for the regions of $|\cos\theta_{\Lambda/\bar{\Lambda}}| > 0.9$ for the differential cross sections of $\Lambda p \rightarrow \Lambda p$ and $\bar{\Lambda} p \rightarrow \bar{\Lambda} p$ to determine the total elastic cross sections. For the reaction $\Lambda p \rightarrow \Lambda p$, we assume the differential cross sections in $-1.0 < \cos\theta_{\Lambda} < -0.9$ and $0.9 < \cos\theta_{\Lambda} < 1.0$ to be the same as those in neighbouring bins. For the reaction $\bar{\Lambda} p \rightarrow \bar{\Lambda} p$, the differential cross section is fitted using a piecewise polynomial function, which is a constant for $\cos\theta_{\bar{\Lambda}} \leq 0$ and a third-order polynomial function for $\cos\theta_{\bar{\Lambda}} \geq 0$. The differential cross section in the regions of $|\cos\theta_{\bar{\Lambda}}| > 0.9$ is obtained according to the fit function. Therefore, the total elastic cross sections integrated over the full angular region are determined to be $\sigma_t(\Lambda p \rightarrow \Lambda p) = (14.2 \pm 1.8_{\text{stat}} \pm 1.3_{\text{sys}})$ mb and $\sigma_t(\bar{\Lambda} p \rightarrow \bar{\Lambda} p) = (27.4 \pm 3.2_{\text{stat}} \pm 2.5_{\text{sys}})$ mb. The result of the total elastic cross section on the reaction $\Lambda p \rightarrow \Lambda p$ is consistent with those measured from other experiments [10–12, 31–42]. The strong forward rise of the differential cross section of $\bar{\Lambda} p \rightarrow \bar{\Lambda} p$ is compatible with the expectation for the case of scattering in

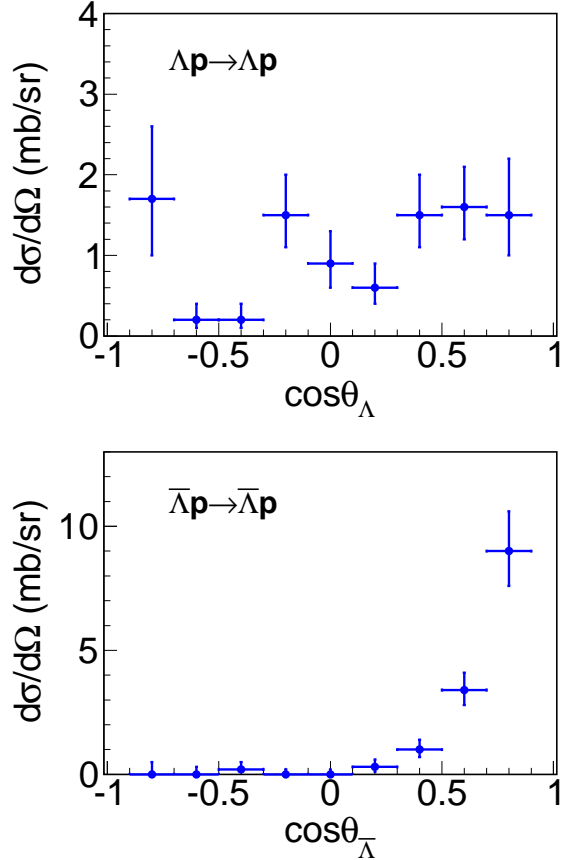


FIG. 3. Differential cross sections of the reactions $\Lambda p \rightarrow \Lambda p$ (top) and $\bar{\Lambda} p \rightarrow \bar{\Lambda} p$ (bottom) at the $\Lambda/\bar{\Lambda}$ momentum of around 1.074 GeV/ c .

the presence of a strong absorption [43–45], which is given by the annihilation part of the potential. Especially, this behavior is very similar to $\bar{p}p$ elastic scattering in a comparable incident momentum region [44], in contrast, such a strong forward rise does not appear in $p\bar{p}$ elastic scattering [46]. This indicates that the strong absorption mechanism is not only important in $\bar{N}N$ scattering, but also in $\bar{Y}N$ scattering. If we assume the reaction $\bar{\Lambda} p \rightarrow \bar{\Lambda} p$ is a pure “black sphere” scattering, the total elastic cross section is given by $\sigma_t(\bar{\Lambda} p \rightarrow \bar{\Lambda} p) = \pi R^2$ [43], where R is the interaction radius. This gives $R = (0.93 \pm 0.07)$ fm, which is comparable to the proton radius [1].

The sources of systematic uncertainties related to the measured cross sections are discussed in the following. The uncertainties in the tracking efficiency and PID efficiency are 1% per track [23]. The uncertainty of the track number requirement is estimated with the control sample $J/\psi \rightarrow \Lambda\bar{\Lambda} \rightarrow p\pi^- \bar{p}\pi^+$. The uncertainties for the branching fractions are taken from the PDG [1]. To estimate the uncertainty from the position of the e^+e^- interaction point, we change the integral range by ± 0.1 cm, which is from (a, b) to $(a+0.1, b+0.1)$ or $(a-0.1, b-0.1)$,

and the larger difference in the result is taken as the uncertainty. The systematic uncertainties from $\Lambda/\bar{\Lambda}$ mass windows, $M_{\text{recoil}}(\bar{\Lambda}p_\Lambda)/M_{\text{recoil}}(\Lambda\bar{p})$ requirement, R_{xy} requirement and $P(p_{\text{oil}})$ requirement are tested using a Barlow test method [24], and these items can be considered negligible. The systematic uncertainties from the fit procedure, the number of J/ψ events, the angular distribution of $J/\psi \rightarrow \Lambda\bar{\Lambda}$ and the Λ mean lifetime are all less than 1% and can be ignored. A summary of the main systematic uncertainties is presented in Table III, and the total systematic uncertainty is obtained by adding all the individual components in quadrature.

TABLE III. Summary of systematic uncertainties (in %).

Source	$\sigma(\Lambda p \rightarrow \Lambda p/\bar{\Lambda}p \rightarrow \bar{\Lambda}p)$
Tracking efficiency	5.0
PID efficiency	5.0
Track number	2.2
Branching fractions	4.9
e^+e^- interaction point	2.0
sum	9.1

In summary, using $(10.087 \pm 0.044) \times 10^9$ J/ψ events collected with the BESIII detector operating at the BEPCII storage ring, the reactions $\Lambda p \rightarrow \Lambda p$ and $\bar{\Lambda}p \rightarrow \bar{\Lambda}p$ are measured, where $\Lambda/\bar{\Lambda}$ are from the process $J/\psi \rightarrow \Lambda\bar{\Lambda}$ and p is from the cooling oil in the beam pipe. The cross sections in $-0.9 \leq \cos\theta_{\Lambda/\bar{\Lambda}} \leq 0.9$ are measured to be $\sigma(\Lambda p \rightarrow \Lambda p) = (12.2 \pm 1.6_{\text{stat}} \pm 1.1_{\text{sys}})$ mb and $\sigma(\bar{\Lambda}p \rightarrow \bar{\Lambda}p) = (17.5 \pm 2.1_{\text{stat}} \pm 1.6_{\text{sys}})$ mb at the $\Lambda/\bar{\Lambda}$ momentum of $1.074 \text{ GeV}/c$ within a range of $\pm 0.017 \text{ GeV}/c$. Furthermore, the differential cross sections of the two reactions are also measured. There is a slight tendency of forward scattering for $\Lambda p \rightarrow \Lambda p$, while a strong forward peak for $\bar{\Lambda}p \rightarrow \bar{\Lambda}p$ is observed. If we make an extrapolation for the regions of $|\cos\theta_{\Lambda/\bar{\Lambda}}| > 0.9$ for the differential cross sections of $\Lambda p \rightarrow \Lambda p$ and $\bar{\Lambda}p \rightarrow \bar{\Lambda}p$, the total elastic cross sections integrated over the full angular region are determined to be $\sigma_t(\Lambda p \rightarrow \Lambda p) = (14.2 \pm 1.8_{\text{stat}} \pm 1.3_{\text{sys}})$ mb and $\sigma_t(\bar{\Lambda}p \rightarrow \bar{\Lambda}p) = (27.4 \pm 3.2_{\text{stat}} \pm 2.5_{\text{sys}})$ mb. These constitute the first result of $\bar{Y}N$ scattering, and will serve as input for the theoretical understanding of the (anti)hyperon-nucleon interaction. This work is the first study of (anti)hyperon-nucleon elastic scattering at an electron-positron collider, and demonstrates the feasibility for studying other antihyperons, such as $\bar{\Sigma}p \rightarrow \bar{\Sigma}p$ and $\bar{\Xi}p \rightarrow \bar{\Xi}p$. The momentum dependence of these cross sections could be studied at a future super tau-charm factory [47, 48] by exploiting multi-body processes or other charmonium decays.

The BESS Collaboration thanks the staff of BEPCII and the IHEP computing center for their strong support. This work is supported in part by National Key R&D Program of China under Contracts Nos. 2020YFA0406300, 2020YFA0406400; National Natural

Science Foundation of China (NSFC) under Contracts Nos. 12375071, 11635010, 11735014, 11835012, 11935015, 11935016, 11935018, 11961141012, 12025502, 12035009, 12035013, 12061131003, 12192260, 12192261, 12192262, 12192263, 12192264, 12192265, 12221005, 12225509, 12235017; Natural Science Foundation of Henan under Contract No. 242300421163; the Chinese Academy of Sciences (CAS) Large-Scale Scientific Facility Program; the CAS Center for Excellence in Particle Physics (CCEPP); Joint Large-Scale Scientific Facility Funds of the NSFC and CAS under Contract No. U1832207; CAS Key Research Program of Frontier Sciences under Contracts Nos. QYZDJ-SSW-SLH003, QYZDJ-SSW-SLH040; 100 Talents Program of CAS; The Institute of Nuclear and Particle Physics (INPAC) and Shanghai Key Laboratory for Particle Physics and Cosmology; European Union's Horizon 2020 research and innovation programme under Marie Skłodowska-Curie grant agreement under Contract No. 894790; German Research Foundation DFG under Contracts Nos. 455635585, Collaborative Research Center CRC 1044, FOR5327, GRK 2149; Istituto Nazionale di Fisica Nucleare, Italy; Ministry of Development of Turkey under Contract No. DPT2006K-120470; National Research Foundation of Korea under Contract No. NRF-2022R1A2C1092335; National Science and Technology fund of Mongolia; National Science Research and Innovation Fund (NSRF) via the Program Management Unit for Human Resources & Institutional Development, Research and Innovation of Thailand under Contract No. B16F640076; Polish National Science Centre under Contract No. 2019/35/O/ST2/02907; The Swedish Research Council; U. S. Department of Energy under Contract No. DE-FG02-05ER41374.

-
- [1] R. L. Workman *et al.* [Particle Data Group], *PTEP* **2022**, 083C01 (2022).
 - [2] J. Adams *et al.* [STAR Collaboration], *Phys. Rev. C* **74**, 064906 (2006).
 - [3] J. Adam *et al.* [STAR Collaboration], *Phys. Lett. B* **790**, 490 (2019).
 - [4] S. Acharya *et al.* [ALICE Collaboration], *Phys. Rev. Lett.* **123**, 112002 (2019).
 - [5] S. Acharya *et al.* [ALICE Collaboration], *Nature* **588**, 232 (2020).
 - [6] E. Botta, T. Bressani and G. Garbarino, *Eur. Phys. J. A* **48**, 41 (2012).
 - [7] A. Gal, E. V. Hungerford and D. J. Millener, *Rev. Mod. Phys.* **88**, 035004 (2016).
 - [8] E. Hiyama and K. Nakazawa, *Ann. Rev. Nucl. Part. Sci.* **68**, 131 (2018).
 - [9] S. H. Hayakawa *et al.* [J-PARC E07 Collaboration], *Phys. Rev. Lett.* **126**, 062501 (2021).
 - [10] G. Alexander, U. Karshon, A. Shapira, G. Yekutieli, R. Engelmann, H. Filthuth and W. Lughofer, *Phys. Rev.* **173**, 1452 (1968).

- [11] B. Sechi-Zorn, B. Kehoe, J. Twitty and R. A. Burnstein, *Phys. Rev.* **175**, 1735 (1968).
- [12] J. A. Kadyk, G. Alexander, J. H. Chan, P. Gaposchkin and G. H. Trilling, *Nucl. Phys. B* **27**, 13 (1971).
- [13] I. Vidaña, *Nucl. Phys. A* **914**, 367 (2013).
- [14] D. Chatterjee and I. Vidaña, *Eur. Phys. J. A* **52**, 29 (2016).
- [15] I. Vidaña, *Proc. Roy. Soc. Lond. A* **474**, 0145 (2018).
- [16] L. Tolos and L. Fabbietti, *Prog. Part. Nucl. Phys.* **112**, 103770 (2020).
- [17] D. Lonardoni, A. Lovato, S. Gandolfi and F. Pederiva, *Phys. Rev. Lett.* **114**, 092301 (2015).
- [18] J. Haidenbauer, U. G. Meißner and A. Nogga, *Eur. Phys. J. A* **56**, 91 (2020).
- [19] C. H. Yu *et al.*, Proceedings of IPAC2016, Busan, Korea, 2016, doi: [10.18429/JACoW-IPAC2016-TUYA01](https://doi.org/10.18429/JACoW-IPAC2016-TUYA01).
- [20] M. Ablikim *et al.* [BESIII Collaboration], *Nucl. Instrum. Meth. A* **614**, 345 (2010).
- [21] M. Ablikim *et al.* [BESIII Collaboration], *Chin. Phys. C* **46**, 074001 (2022).
- [22] P. D. Barnes *et al.*, Ettore Majorana International Science Series, vol 17, Springer, Boston, MA, 1984, doi:[10.1007/978-1-4684-8727-5_46](https://doi.org/10.1007/978-1-4684-8727-5_46).
- [23] M. Ablikim *et al.* [BESIII Collaboration], *Phys. Rev. Lett.* **130**, 251902 (2023).
- [24] M. Ablikim *et al.* [BESIII Collaboration], arXiv: [2310.00720](https://arxiv.org/abs/2310.00720).
- [25] S. Agostinelli *et al.* [GEANT4 Collaboration], *Nucl. Instrum. Meth. A* **506**, 250 (2003).
- [26] S. Jadach, B. F. L. Ward and Z. Was, *Phys. Rev. D* **63**, 113009 (2001); *Comput. Phys. Commun.* **130**, 260 (2000).
- [27] D. J. Lange, *Nucl. Instrum. Meth. A* **462**, 152 (2001); R. G. Ping, *Chin. Phys. C* **32**, 599 (2008).
- [28] J. C. Chen, G. S. Huang, X. R. Qi, D. H. Zhang and Y. S. Zhu, *Phys. Rev. D* **62**, 034003 (2000); R. L. Yang, R. G. Ping and H. Chen, *Chin. Phys. Lett.* **31**, 061301 (2014).
- [29] E. Richter-Was, *Phys. Lett. B* **303**, 163 (1993).
- [30] M. Ablikim *et al.* [BESIII Collaboration], *Phys. Rev. Lett.* **129**, 131801 (2022).
- [31] F. Crawford, Jr., M. Cresti, M. Good, F. Solmitz, M. Stevenson and H. Ticho, *Phys. Rev. Lett.* **2**, 174 (1959).
- [32] G. Alexander, J. A. Anderson, F. S. Crawford, Jr., W. Laskar and L. J. Lloyd, *Phys. Rev. Lett.* **7**, 346 (1961).
- [33] T. H. Groves, *Phys. Rev.* **129**, 1372 (1963).
- [34] P. Beillière, J. L. Gomez, A. Lloret, A. Roussel, K. Myklebost and J. M. Olsen, *Phys. Lett.* **12**, 350 (1964).
- [35] L. Piekenbrock and F. Oppenheimer, *Phys. Rev. Lett.* **12**, 625 (1964).
- [36] B. Sechi-Zorn, R. A. Burnstein, T. B. Day, B. Kehoe and G. A. Snow, *Phys. Rev. Lett.* **13**, 282 (1964).
- [37] D. Bassano, C. Y. Chang, M. Goldberg, T. Kikuchi and J. Leitner, *Phys. Rev.* **160**, 1239 (1967).
- [38] G. R. Charlton, J. Badier, E. Barrelet, I. Makarovisch, J. Pernegr, J. R. Hubbard, A. Leveque, C. Louedec, L. Moscoso and D. Revel, *Phys. Lett. B* **32**, 720 (1970).
- [39] K. J. Anderson, N. M. Gelfand, J. Keren and T. H. Tan, *Phys. Rev. D* **11**, 473 (1975).
- [40] R. P. Mount, R. E. Ansorge, J. R. Carter, W. W. Neale, J. G. Rushbrooke and D. R. Ward, *Phys. Lett. B* **58**, 228 (1975).
- [41] J. M. Hauptman, J. A. Kadyk and G. H. Trilling, *Nucl. Phys. B* **125**, 29 (1977).
- [42] J. Rowley *et al.* [CLAS Collaboration], *Phys. Rev. Lett.* **127**, 272303 (2021).
- [43] C. A. Coombes, B. Cork, W. Galbraith, G. R. Lambertson and W. A. Wenzel, *Phys. Rev.* **112**, 1303 (1958).
- [44] D. L. Parker, B. Y. Oh, G. A. Smith and R. J. Sprafka, *Nucl. Phys. B* **32**, 29 (1971).
- [45] P. Schiavon *et al.*, *Nucl. Phys. A* **505**, 595 (1989).
- [46] M. G. Albrow *et al.*, *Nucl. Phys. B* **23**, 445 (1970).
- [47] A. E. Bondar *et al.* [Charm-Tau Factory Collaboration], *Phys. Atom. Nucl.* **76**, 1072 (2013).
- [48] M. Achasov *et al.*, *Front. Phys.* **19**, 14701 (2024).